

## Mechanisms of injection enhancement in organic light-emitting diodes through insulating buffer

J. M. Zhao, Y. Q. Zhan, S. T. Zhang, X. J. Wang, Y. C. Zhou, Y. Wu, Z. J. Wang, X. M. Ding, and X. Y. Hou<sup>a)</sup>

Surface Physics Laboratory (National Key Laboratory), Institute of Advanced Materials, Fudan University, Shanghai 200433, China

(Received 6 January 2004; accepted 28 April 2004; published online 17 June 2004)

Three types of organic light-emitting diodes are fabricated. Tris-8-hydroxyquinoline aluminum ( $\text{Alq}_3$ ) is used as an electron-transporting layer (ETL) and sodium stearate (NaSt) as an electron-injecting buffer. The optimal thickness of NaSt for electron injection is different for cathodes of different metals, such as Mg, Al, and Ag. This is attributed to the different work functions of cathodes, which result in different initial barrier heights for electron injection from cathodes into ETL, and explained based on tunneling theory. © 2004 American Institute of Physics. [DOI: 10.1063/1.1764943]

Highly efficient injection of carriers from electrodes is needed for the development of high-performance organic light-emitting diodes (OLEDs).<sup>1-13</sup> In 1997, the introduction of LiF into OLEDs was proved to be an effective way for improving electron injection from Al into tris-8-hydroxyquinoline aluminum ( $\text{Alq}_3$ ).<sup>1</sup> Thereafter, it has been found that many insulators with proper thicknesses, including  $\text{MgF}_2$ ,<sup>1</sup> NaCl,<sup>2</sup> CsF,<sup>3</sup> and  $\text{Al}_2\text{O}_3$ ,<sup>4</sup> have similar effects on electron injection into a variety of organic semiconductors. Meanwhile it has been shown that besides electron, hole injection could also be enhanced by introducing insulating buffers at some interfaces.<sup>5-7</sup>

In general, it is believed that the similar characteristics of devices with different insulating buffers should result from similar mechanism.<sup>7,8,10-12</sup> The debate on the mechanism has mainly focused on two models. One is tunneling probability enhancement resulting from buffer-induced energy level realignment,<sup>7,9-12</sup> the other is the chemical reaction model,<sup>13-15</sup> by which it is thought alkali atoms or alkali-earth atoms in the compounds (e.g., LiF, CsF) adopted are liberated and improve the electron injection due to their low work functions. However, the chemical reaction model is unable to explain the buffer-induced hole injection enhancement,<sup>5-7</sup> because such metals would reduce the hole injection. Meanwhile, even for electron injection it is inapplicable to the cases of  $\text{Al}_2\text{O}_3$  (Ref. 4) and PMMA,<sup>9</sup> which do not contain any metal atoms with low work function. Additionally, in terms of chemical reaction model Hung *et al.*<sup>14</sup> found that in the ternary system of Ag/LiF/ $\text{Alq}_3$  the release of Li is thermodynamically inhibited and hence concluded that LiF could not enhance the electron injection from Ag to  $\text{Alq}_3$ . Such a conclusion was also drawn by Heil *et al.*<sup>15</sup> experimentally. However, it was demonstrated recently that LiF with 3.0 nm thickness could greatly enhance the electron injection from Ag to  $\text{Alq}_3$ .<sup>10</sup>

Before LiF was introduced into OLEDs, Kim *et al.*<sup>9</sup> had demonstrated that insertion of Langmuir-Blodgett films of poly(methyl methacrylate) (PMMA) between Al and poly[2-methoxy-5-(2-ethylhexyloxy)-1,4-phenylene-vinylene] (MEHPPV) resulted in enhanced quan-

tum efficiency in polymer EL devices and given an explanation in terms of the tunneling model. Recently, Zhang *et al.*<sup>11</sup> at this laboratory made detailed calculations based on tunneling model, showing that various parameters, such as the resistivity ratio of buffer to organic layer, position of the conduction band minimum of the buffer relative to the lowest unoccupied molecular orbital (LUMO) of the organic layer and the thicknesses of both layers, may affect the electron injection in the system of cathode/buffer/organic layer. More recently, it was demonstrated that the introduction of LiF between indium-tin-oxide (ITO) and *N,N'*-bis(1-naphthyl)-*N,N'*-diphenyl-1,1'-biphenyl 4,4'-dimaine (NPB) can enhance hole injection or not is dependent on the initial barrier height (IBH) for hole injection from ITO into NPB.<sup>7</sup> For large IBH (the ITO used is treated by  $\text{H}_2$ -plasma and hence has low work function resulting in large IBH for hole injection),<sup>16</sup> LiF greatly enhances the hole injection; for small one (the ITO is treated by UV ozone and hence has high work function resulting in small IBH for hole injection),<sup>16</sup> however, it will weaken the hole injection. Additionally, it has also been found that in the case of LiF-induced hole injection the optimal thickness of the buffer layer is dependent on the values of IBHs. The larger the IBH is, the larger the optimal thickness will be. Such behaviors have been explained based on the tunneling model.

In this letter, it is demonstrated experimentally that the optimal thickness of sodium stearate (NaSt) as an electron-injecting buffer at cathode side also depends on the IBH at the interface of the cathode/electron-transporting layer (ETL). The optimal thickness of NaSt increases with IBH. These phenomena indicate that the mechanism of NaSt-induced electron injection enhancement in OLEDs is not a chemical reaction but energy level alignment and tunneling.

Three types of OLEDs with the same structure, i.e., cathode/NaSt (with varied thickness)/ $\text{Alq}_3$  (65 nm)/NPB (65 nm)/ITO, were fabricated, named, respectively, Mg-OLEDs, Al-OLEDs, and Ag-OLEDs corresponding to the use of Mg\Ag, Al and Ag as cathode. The details of sample fabrication and measurement of current density-luminescence-voltage (*I-L-V*) characteristics are shown elsewhere.<sup>7</sup>

<sup>a)</sup>Electronic-mail: xyhou@fudan.edu.cn

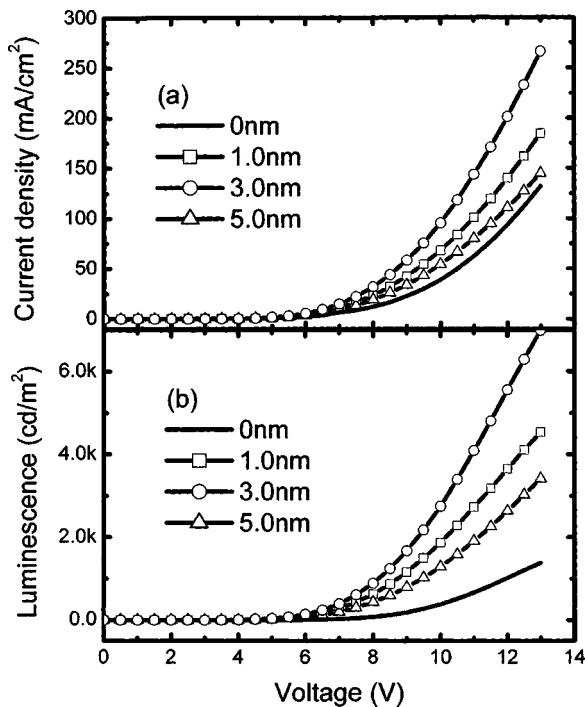


FIG. 1.  $I-V$  (a) and  $B-V$  (b) curves measured from Al-OLEDs with a NaSt buffer of various thicknesses.

Zhan *et al.*<sup>12</sup> at this laboratory have shown the effect of NaSt on electron injection in OLEDs and an optimal thickness of 3.0 nm for NaSt-enhanced electron injection was obtained. For the integrality of the experimental data in this study, we repeated the experiments with the device structure of ITO\NPB\Alq<sub>3</sub>NaSt\Al and obtained the same results. Figure 1 shows the  $I-V$  and  $L-V$  curves of Al-OLEDs. It can be seen that a thin (1.0 nm) layer of NaSt enhances not only the current injection but also the brightness. A 3.0 nm NaSt shows the optimal effects and a 5.0 nm one shows the degradation of current injection and EL output. So, the NaSt optimal thickness of 3.0 nm is also obtained for Al-OLEDs here.

Figure 2 shows the  $I-V$  and  $L-V$  curves of Mg-OLEDs, in which the electron is injected through Mg because Mg contacts directly with NaSt (or Alq<sub>3</sub>) for Mg\Ag

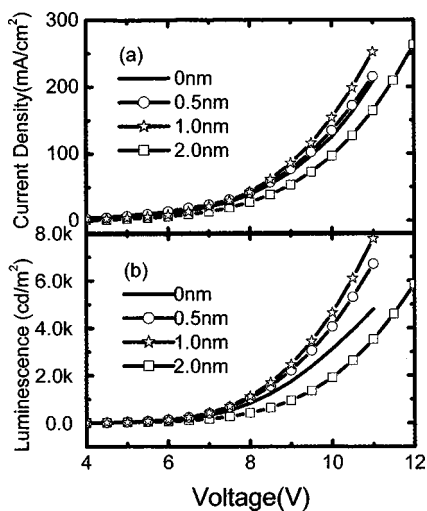


FIG. 2.  $I-V$  (a) and  $B-V$  (b) curves measured from Mg-OLEDs with a NaSt buffer of various thicknesses.

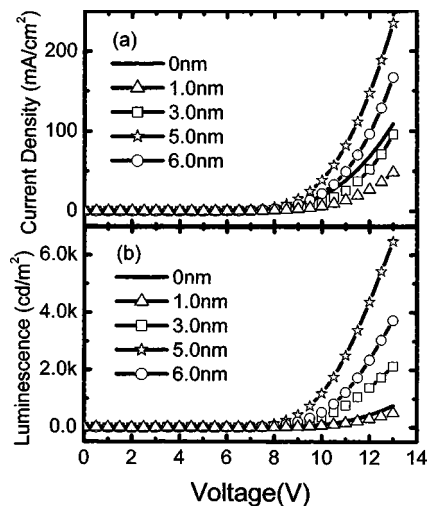


FIG. 3.  $I-V$  (a) and  $B-V$  (b) curves measured from Ag-OLEDs with a NaSt buffer of various thicknesses.

composite cathode. As can be seen, such type of device is different from Al-OLEDs. The current injection is slightly enhanced by the layers of 0.5 and 1.0 nm NaSt (the 1.0 nm layer even looks better) but evidently deteriorated by 2.0 nm layer. From Fig. 2 it is considered that the optimal thickness of NaSt for electron injection from Mg to Alq<sub>3</sub> is about 1.0 nm.

Figure 3 shows the  $I-V$  and  $L-V$  curves of Ag-OLEDs. Different from the above mentioned cases, with a 1.0 nm NaSt layer inserted between Alq<sub>3</sub> and Ag, both  $I-V$  and  $L-V$  curves are shifted toward high voltage region compared with the device without NaSt. Further increasing the NaSt layer thickness (3.0 nm), current injection of the device is gradually enhanced. When the thickness of NaSt is increased to 5.0 nm, the device shows optimal current injection and EL output. The NaSt layer thickness over 5.0 nm shifts the  $I-V$  and  $L-V$  curves back to the higher voltage region. Similar phenomenon has also been observed in the case of Ag/LiF/Alq<sub>3</sub> and a qualitative explanation on it was given.<sup>10</sup> In short, compared with the cases of Al-OLEDs and Mg-OLEDs, a large optimal thickness of NaSt (5.0 nm) for electron injection from Ag to Alq<sub>3</sub> is definitely observed.

The optimal thickness of NaSt for electron injection versus the IBH between  $E_F$  of different cathode and LUMO of Alq<sub>3</sub> are plotted in Fig. 4. The work functions of Mg, Al, and

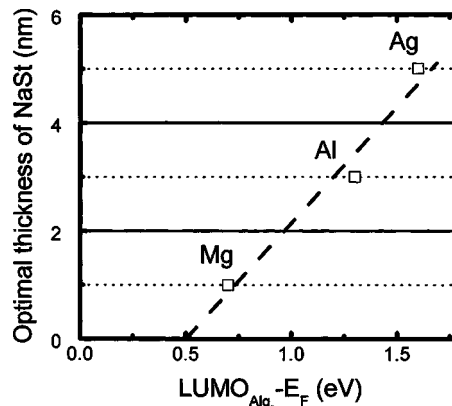


FIG. 4. Optimal thickness of NaSt for electron injection vs the initial barrier height between Fermi level ( $E_F$ ) of cathode and LUMO of Alq<sub>3</sub>. The dashed line is a guide for the eye.

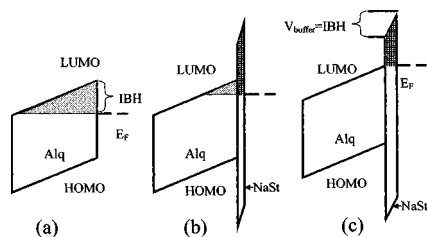


FIG. 5. Schematic diagram of the tunneling model without and with a NaSt buffer.  $V_{\text{buffer}}$  denotes the voltage drop across NaSt buffer layer in the case of optimal thickness of NaSt.

Ag are about 3.7, 4.3, and 4.6 eV,<sup>17</sup> respectively, and the LUMO of Alq<sub>3</sub> is about 3.0 eV below the vacuum level.<sup>12</sup> Therefore, the IBH of Mg-OLEDs, Al-OLEDs, and Ag-OLEDs are about 0.7, 1.3, and 1.6 eV, respectively. It can be clearly seen in Fig. 4 that the optimal thickness of NaSt increases with IBH. A tentative dashed line to guide the eye is drawn through the three experimental points. Noticeably, the line intersects the abscissa axis at (0.5, 0), which might be an indication that for an IBH less than 0.5 eV no buffer will be needed for the optimal injection. Interestingly, as mentioned previously, it has been found that an insulating buffer (LiF) even with optimal thickness can hardly enhance the hole injection at ITO\NPB interface with about 0.5 eV IBH for hole injection; on the contrary, the hole injection can be greatly enhanced by introducing the same buffer at ITO\NPB interface with larger IBH.<sup>7</sup>

The dependence of buffer thickness on IBH can be understood based on a simple tunneling model, which is schematically shown in Fig. 5. If no buffer layer is included, upon application of a forward voltage the electron must tunnel through the shaded triangle barrier, as shown in Fig. 5(a). The presence of a thin layer of buffer has two effects: (i) the voltage drop across it lifts the cathode  $E_F$  by the same amount and hence reduces the triangle barrier in Alq<sub>3</sub> layer, as shown in Fig. 5(b); (ii) the buffer layer adds an additional barrier formed by itself, the area with reticulation, as shown in Figs. 5(b) and 5(c). If the total effective barrier with proper-thickness NaSt, including the shaded area and reticulation area, is lowered compared with the case of no buffer, the presence of NaSt buffer will enhance the electron injection from cathode into Alq<sub>3</sub>. Optimal thickness may be achieved when electrons tunneling through the buffer layer encounter no further barrier during crossing the organic layer, i.e., that the position of  $E_F$  of cathode and LUMO of organic layer are aligned to each other, as shown in Fig. 5(c). In such a case, the value of potential drop across the buffer layer is equal to that of the IBH between  $E_F$  of cathode and LUMO of organic layer. Based on this, to align larger barrier height, larger potential drop across the buffer is needed at a given voltage, and hence the buffer layer should be thicker. Therefore, the optimal thickness will increase with IBH, as observed.

Two assumptions are applied in this model. One is that the electron injection is governed only magnitude of barrier at cathode/ETL; the other is that ohmic law is valid for potential distribution across organic and buffer layers.<sup>11</sup> From Fig. 4 it can be found that the optimal thickness of NaSt shown experimentally for three types of OLEDs is not

as expected, i.e., linear to the IBH, according to the model. This indicates the model is very simple. However, it is sufficiently helpful to qualitatively understand the experimental phenomena.

As the most-investigated buffer in OLEDs, LiF shows quite different optimal thickness at different interfaces,<sup>1,7,10,18–20</sup> the range of which varies from several angstroms to several nanometers. Although these results were reported by different groups, it can be believed that such a large difference results not from the experimental error but an intrinsic reason. The present experiments might be helpful to give a qualitative explanation to those phenomena.

In conclusion, we have shown the dependence of optimal thickness of NaSt for electron injection on IBH between ETL and different cathodes. The larger the IBH is, the larger the optimal thickness will be. This is attributed to the different work functions of cathodes, which result in different initial barrier heights for electron injection from cathodes into ETL, and can be understood based on tunneling model.

This work is supported by the CNKBRFSF, the National Natural Science Foundation of China under Grant No. 10174013, and the Science and Technology Commission of Shanghai Municipality.

<sup>1</sup>L. S. Hung, C. W. Tang, and M. G. Mason, *Appl. Phys. Lett.* **70**, 152 (1997).

<sup>2</sup>S. J. Kang, D. S. Park, S. Y. Kim, C. N. Whang, K. Jeong, and S. Im, *Appl. Phys. Lett.* **81**, 2581 (2002).

<sup>3</sup>P. Piromreun, H. S. Oh, Y. Shen, G. G. Malliaras, J. Campbell Scott, and P. J. Brock, *Appl. Phys. Lett.* **77**, 2403 (2000).

<sup>4</sup>F. Li, H. Tang, J. Anderegg, and J. Shinar, *Appl. Phys. Lett.* **70**, 1233 (1997).

<sup>5</sup>F. Zhu, B. Low, K. Zhang, and S. Chua, *Appl. Phys. Lett.* **79**, 1205 (2001).

<sup>6</sup>Y. Zhao, S. Y. Liu, and J. Y. Hou, *Thin Solid Films* **397**, 208 (2001).

<sup>7</sup>J. M. Zhao, S. T. Zhang, X. J. Wang, Y. Q. Zhan, X. Z. Wang, G. Y. Zhong, Z. J. Wang, X. M. Ding, W. Huang, and X. Y. Hou, *Appl. Phys. Lett.* **84**, 2913 (2004).

<sup>8</sup>J. Yoon, J. J. Kim, T. W. Lee, and O. O. Park, *Appl. Phys. Lett.* **76**, 2152 (2000).

<sup>9</sup>Y. E. Kim, H. Park, and J. J. Kim, *Appl. Phys. Lett.* **69**, 599 (1996).

<sup>10</sup>X. J. Wang, J. M. Zhao, Y. C. Zhou, X. Z. Wang, S. T. Zhang, Y. Q. Zhan, Z. Xu, H. J. Ding, G. Y. Zhong, H. Z. Shi, Z. H. Xiong, Y. Liu, Z. J. Wang, E. G. Obbard, X. M. Ding, W. Huang, and X. Y. Hou, *J. Appl. Phys.* **95**, 3828 (2004).

<sup>11</sup>S. T. Zhang, X. M. Ding, J. M. Zhao, H. Z. Shi, J. He, Z. H. Xiong, H. J. Ding, E. G. Obbard, Y. Q. Zhan, W. Huang, and X. Y. Hou, *Appl. Phys. Lett.* **84**, 425 (2004).

<sup>12</sup>Y. Q. Zhan, Z. H. Xiong, H. Z. Shi, S. T. Zhang, Z. Xu, G. Y. Zhong, J. He, J. M. Zhao, Z. J. Wang, E. Obbard, H. J. Ding, X. J. Wang, X. M. Ding, W. Huang, and X. Y. Hou, *Appl. Phys. Lett.* **83**, 1656 (2003).

<sup>13</sup>G. Mason, C. W. Tang, L. S. Hung, P. Raychaudhuri, J. Madathil, D. J. Giesen, L. Yan, Q. T. Le, Y. Gao, S. T. Lee, L. S. Liao, L. F. Cheng, W. R. Salaneck, D. A. dos Santos, and J. L. Bredas, *J. Appl. Phys.* **89**, 2756 (2001).

<sup>14</sup>L. S. Hung, R. Q. Zhang, P. He, and G. Mason, *J. Phys. D* **35**, 103 (2002).

<sup>15</sup>H. Heil, J. Steiger, S. Karg, M. Gastel, H. Orther, and H. von Seggem, *J. Appl. Phys.* **89**, 420 (2001).

<sup>16</sup>C. C. Wu, C. I. Wu, J. C. Sturm, and A. Kahn, *Appl. Phys. Lett.* **70**, 1348 (1997).

<sup>17</sup>I. D. Parker, *J. Appl. Phys.* **75**, 1656 (1994).

<sup>18</sup>T. M. Brown, R. H. Friend, I. S. Millard, D. J. Lacey, J. H. Burroughes, and F. Cacialli, *Appl. Phys. Lett.* **79**, 174 (2001).

<sup>19</sup>G. E. Jabbour, Y. Kawabe, S. E. Shaheen, J. F. Wang, M. M. Morrell, B. Kippelen, and N. Peyghambarian, *Appl. Phys. Lett.* **71**, 1762 (1997).

<sup>20</sup>T. M. Brown, I. S. Millard, D. J. Lacey, J. H. Burroughes, R. H. Friend, and F. Cacialli, *Synth. Met.* **124**, 15 (2000).